# Migration of mode-converted seismic data

*A.J. Berkhout*, C.P.A. Wapenaar and D.J. Verschuur,*
*Centre for Technical Geoscience, Laboratory of Seismics and Acoustics, Delft Univ. of Technology*

**Summary**

In this paper we extend the Common Focus Point (CFP) processing technique [2] to mode-converted data. We show that, by introducing minor simplifications, the different data types can be migrated independently in exactly the same manner as in the acoustic situation.

**WRW-model for multi-component data**

It has been shown that the $WRW$-model for compressional waves [1] can be logically extended to converted and shear waves [3], according to

$$\mathbf{V} = \mathbf{D}^{-}\mathbf{P}\mathbf{D}^{+}, \tag{1}$$

where

$$\mathbf{P} = \mathbf{W}\mathbf{R}\mathbf{W}\mathbf{S}, \tag{2}$$

or

$$\begin{pmatrix} \mathbf{P}_{p,p} & \mathbf{P}_{p,s} \\ \mathbf{P}_{s,p} & \mathbf{P}_{s,s} \end{pmatrix} = \begin{pmatrix} \mathbf{W}_{p,p} & \mathbf{W}_{p,s} \\ \mathbf{W}_{s,p} & \mathbf{W}_{s,s} \end{pmatrix} \times \begin{pmatrix} \mathbf{R}_{p,p} & \mathbf{R}_{p,s} \\ \mathbf{R}_{s,p} & \mathbf{R}_{s,s} \end{pmatrix} \begin{pmatrix} \mathbf{W}_{p,p} & \mathbf{W}_{p,s} \\ \mathbf{W}_{s,p} & \mathbf{W}_{s,s} \end{pmatrix} \begin{pmatrix} \mathbf{S}_{p} & \mathbf{O} \\ \mathbf{O} & \mathbf{S}_{s} \end{pmatrix}. \tag{3}$$

Here $\mathbf{V}$ and $\mathbf{P}$ represent the multi-component data matrices in terms of particle velocities and potentials, respectively. The subscripts $P$ and $S$ in equation (3) refer to the different wave types. The latter equation can be decoupled into a number of independent data models if mode-conversion is ignored either during reflection or during propagation. Hence, this means that we consider *first-order* mode conversion effects only.

*Ignoring mode-conversion during reflection.*

For conventional marine data the main mode conversion may occur during transmission through a hard sea-bottom, i.e. in $\mathbf{W}_{s,p}$ and $\mathbf{W}_{p,s}$. Ignoring the mode-converted reflection matrices $\mathbf{R}_{s,p}$ and $\mathbf{R}_{p,s}$, setting the shear sources to zero ($\mathbf{S}_s = \mathbf{O}$), equation (3) yields for $\mathbf{P}_{p,p}$:

$$\mathbf{P}_{p,p} = [\mathbf{W}_{p,p}\mathbf{R}_{p,p}\mathbf{W}_{p,p} + \mathbf{W}_{p,s}\mathbf{R}_{s,s}\mathbf{W}_{s,p}]\mathbf{S}_p. \tag{4}$$

*Ignoring mode-conversion during propagation.*

For soft sea-bottoms and for land-data, conversion during transmission is less important. Ignoring in equation (3) the mode-converted propagation matrices $\mathbf{W}_{s,p}$ and $\mathbf{W}_{p,s}$, four independent equations are obtained, according to

$$\mathbf{P}_{p,p} = [\mathbf{W}_{p,p}\mathbf{R}_{p,p}\mathbf{W}_{p,p}]\mathbf{S}_p, \tag{5}$$
$$\mathbf{P}_{p,s} = [\mathbf{W}_{p,p}\mathbf{R}_{p,s}\mathbf{W}_{s,s}]\mathbf{S}_s, \tag{6}$$
$$\mathbf{P}_{s,p} = [\mathbf{W}_{s,s}\mathbf{R}_{s,p}\mathbf{W}_{p,p}]\mathbf{S}_p, \tag{7}$$
$$\mathbf{P}_{s,s} = [\mathbf{W}_{s,s}\mathbf{R}_{s,s}\mathbf{W}_{s,s}]\mathbf{S}_s. \tag{8}$$

Either equation (4) or the system of equations (5) through (8) can be used as a starting point for CFP-processing, depending on the situation. In the following we only consider the second case. We will assume that elastic decomposition (inversion of equation 1) has been carried out [3].

**Elastic CFP operators**

Analogous to the acoustic CFP method [2], we define elastic focusing operators as the rows and columns of the inverse extrapolation matrices:

1. Operator for focused $P$-detectors at $(x_i, z_m)$: the $i$th row of $\mathbf{F}_{p,p}(z_m, z_0) = \mathbf{W}^{*}_{p,p}(z_m, z_0)$, hence
$$[\vec{F}_i^{\dagger}(z_m, z_0)]_{p,p} = \vec{I}_i^{\dagger}(z_m)\mathbf{W}^{*}_{p,p}(z_m, z_0). \tag{9}$$
2. Operator for focused $S$-detectors at $(x_i, z_m)$: the $i$th row of $\mathbf{F}_{s,s}(z_m, z_0) = \mathbf{W}^{*}_{s,s}(z_m, z_0)$, hence
$$[\vec{F}_i^{\dagger}(z_m, z_0)]_{s,s} = \vec{I}_i^{\dagger}(z_m)\mathbf{W}^{*}_{s,s}(z_m, z_0). \tag{10}$$
3. Operator for focused $P$-sources at $(x_j, z_m)$: the $j$th column of $\mathbf{F}_{p,p}(z_0, z_m) = \mathbf{W}^{*}_{p,p}(z_0, z_m)$, hence
$$[\vec{F}_j(z_0, z_m)]_{p,p} = \mathbf{W}^{*}_{p,p}(z_0, z_m)\vec{I}_j(z_m). \tag{11}$$
4. Operator for focused $S$-sources at $(x_j, z_m)$: the $j$th column of $\mathbf{F}_{s,s}(z_0, z_m) = \mathbf{W}^{*}_{s,s}(z_0, z_m)$, hence
$$[\vec{F}_j(z_0, z_m)]_{s,s} = \mathbf{W}^{*}_{s,s}(z_0, z_m)\vec{I}_j(z_m). \tag{12}$$

Vectors with a dagger (†) denote row vectors and vectors without the dagger denote column vectors; $\vec{I}_i^{\dagger}(z_m)$ denotes a unit row vector with '1' at the $i$th position, $\vec{I}_j(z_m)$ a unit column vector with '1' at the $j$th position.

**Focusing in detection**

Using the operators defined in equations (9) and (10), the equations for elastic focusing in *detection* of the upgoing measured $P$- or $S$-waves are given by

$$[\vec{P}_i^{\dagger}(z_m, z_0)]_{p,p} = [\vec{F}_i^{\dagger}(z_m, z_0)]_{p,p}\mathbf{P}_{p,p}(z_0), \tag{13}$$
$$[\vec{P}_i^{\dagger}(z_m, z_0)]_{p,s} = [\vec{F}_i^{\dagger}(z_m, z_0)]_{p,p}\mathbf{P}_{p,s}(z_0), \tag{14}$$
$$[\vec{P}_i^{\dagger}(z_m, z_0)]_{s,p} = [\vec{F}_i^{\dagger}(z_m, z_0)]_{s,s}\mathbf{P}_{s,p}(z_0), \tag{15}$$
$$[\vec{P}_i^{\dagger}(z_m, z_0)]_{s,s} = [\vec{F}_i^{\dagger}(z_m, z_0)]_{s,s}\mathbf{P}_{s,s}(z_0). \tag{16}$$

For illustration purposes, we simulated multi-component data in the horizontally layered model of Figure 1. We focused the upgoing wave field from one point of the *second* reflector, using

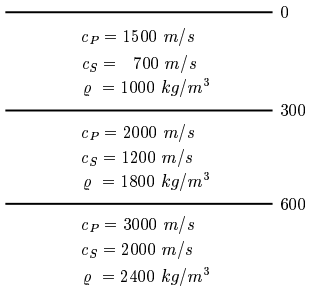


***Fig. 1:*** *Simple elastic model.*

an erroneous macro model with $P$- and $S$-wave velocities in the second layer that are approximately 10% too low. The $P$-$P$ and $P$-$S$ responses are focused with the erroneous $P$-wave CFP operator $[\vec{F}_i^{\dagger}(z_2, z_0)]_{p,p}$ and the $S$-$P$ and $S$-$S$ responses with the erroneous $S$-wave CFP operator $[\vec{F}_i^{\dagger}(z_2, z_0)]_{s,s}$. The resulting four CFP gathers (fixed $x_i$ at $z_2$, variable $x_s$ at $z_0$) are displayed in Figure 2. In this same figure, the traveltimes of the erroneous time reversed operators $[\vec{F}_i^{\dagger}(z_2, z_0)]_{p,p}$ are plotted over the erroneous $P$-$P$ and $S$-$P$ CFP gathers and the traveltimes of the erroneous time reversed operators $[\vec{F}_i^{\dagger}(z_2, z_0)]_{s,s}$ are plotted over the erroneous $P$-$S$ and $S$-$S$ CFP gathers.

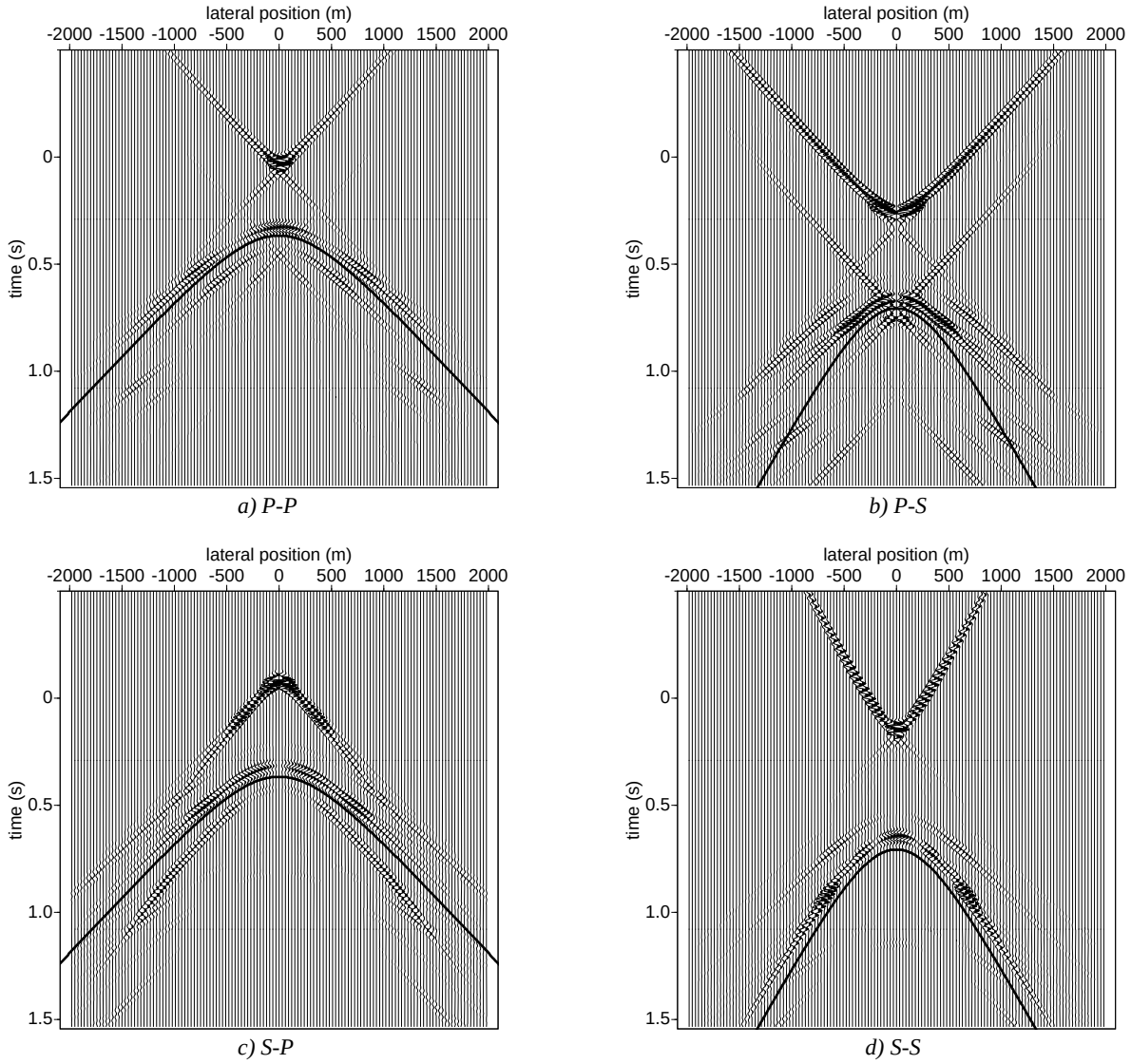


*a) P-P* *b) P-S*

*c) S-P* *d) S-S*

***Fig. 2:*** *Elastic CFP gathers: the result of focusing the upgoing wave field (focusing in detection) onto one gridpoint at the second reflector, using slightly erroneous operators. The operators are shown in this figure as solid curves.*

The small mismatch increases with offset and is due to the errors in the $P$- and $S$-wave velocities. The correct $P$- and $S$-operators are found iteratively by interpolating between the traveltimes in the operators and the corresponding events in the CFP gathers. Note that the actual estimation of the $P$- and $S$-macro models is thus postponed until *after* migration.

**Focusing in emission**

Using the updated operators, the equations for elastic focusing in *emission* of the downgoing induced $P$- or $S$-waves are given by

$$[P_{ij}(z_m)]_{p,p} = [\vec{P}_i^{\dagger}(z_m, z_0)]_{p,p}[\vec{F}_j(z_0, z_m)]_{p,p}, \quad (17)$$

$$[P_{ij}(z_m)]_{p,s} = [\vec{P}_i^{\dagger}(z_m, z_0)]_{p,s}[\vec{F}_j(z_0, z_m)]_{s,s}, \quad (18)$$

$$[P_{ij}(z_m)]_{s,p} = [\vec{P}_i^{\dagger}(z_m, z_0)]_{s,p}[\vec{F}_j(z_0, z_m)]_{p,p}, \quad (19)$$

$$[P_{ij}(z_m)]_{s,s} = [\vec{P}_i^{\dagger}(z_m, z_0)]_{s,s}[\vec{F}_j(z_0, z_m)]_{s,s}. \quad (20)$$

We applied these focusing steps to the updated CFP gathers of Figure 2. The resulting gridpoint functions (fixed $x_j$ at $z_2$ and variable $x_i$ at $z_2$) are shown in Figure 3 and their $\tau, p$-transformed versions in Figure 4. The samples at zero time and zero offset of the gridpoint functions in Figure 3 represent the average reflection coefficients at the chosen gridpoint (output of confocal elastic migration). The cross-sections at zero intercept-time of the gridpoint functions in Figure 4 represent the *angle-dependent* reflection coefficients of the second reflector (output of bifocal elastic migration). Figure 5 shows the extracted reflection amplitudes.

**Conclusions**

The acoustic double focusing process can be easily extended to the elastodynamic situation by introducing focusing operators for $P$- and $S$-wavefields. Errors in the operators can be detected and a simple updating step exists. Elastic CFP migration is suited for conventional marine data, seabottom data as well as land data.

**References**

[1] A. J. Berkhout. *Imaging of acoustic energy by wave field extrapolation (3rd edition).* Elsevier, Amsterdam, 1985.

[2] A. J. Berkhout. Pushing the limits of seismic imaging. Part I. Prestack migration in terms of double dynamic focusing. *Geophysics*, 62:Accepted, 1997.

[3] C. P. A. Wapenaar and A. J. Berkhout. *Elastic wave field extrapolation*. Elsevier Amsterdam, 1989.

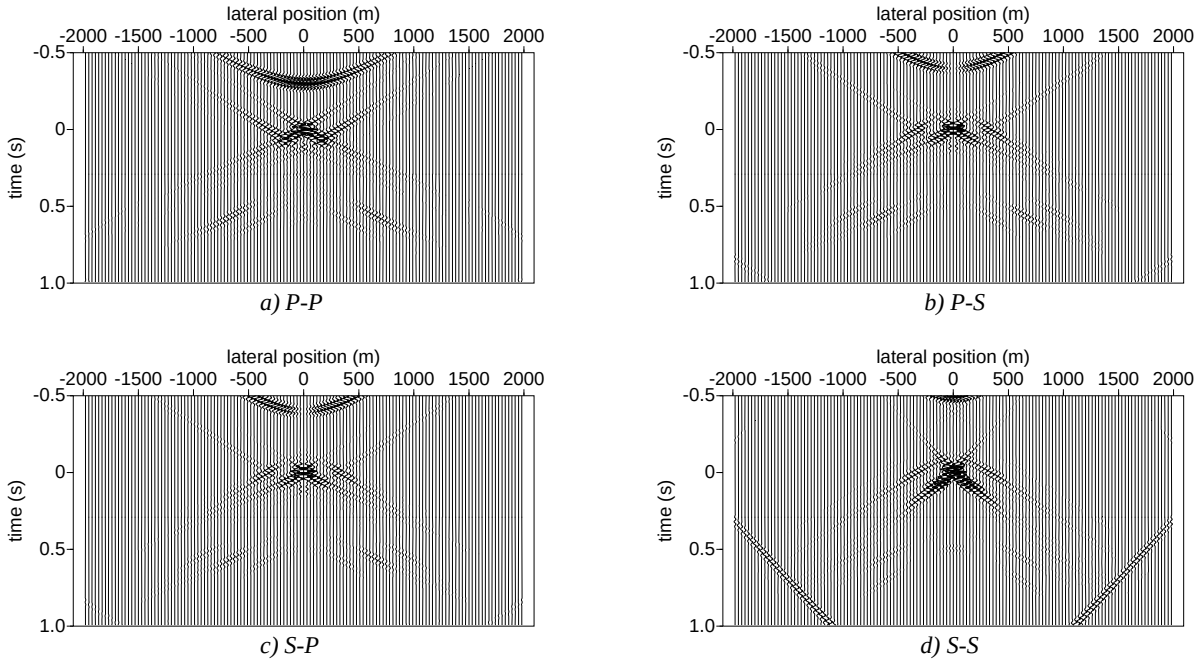


***Fig. 3:*** *Elastic gridpoint functions: the $P$- and $S$-wave sources have been focused on the second reflector, using the correct operators. Note the focused headwave in d).*

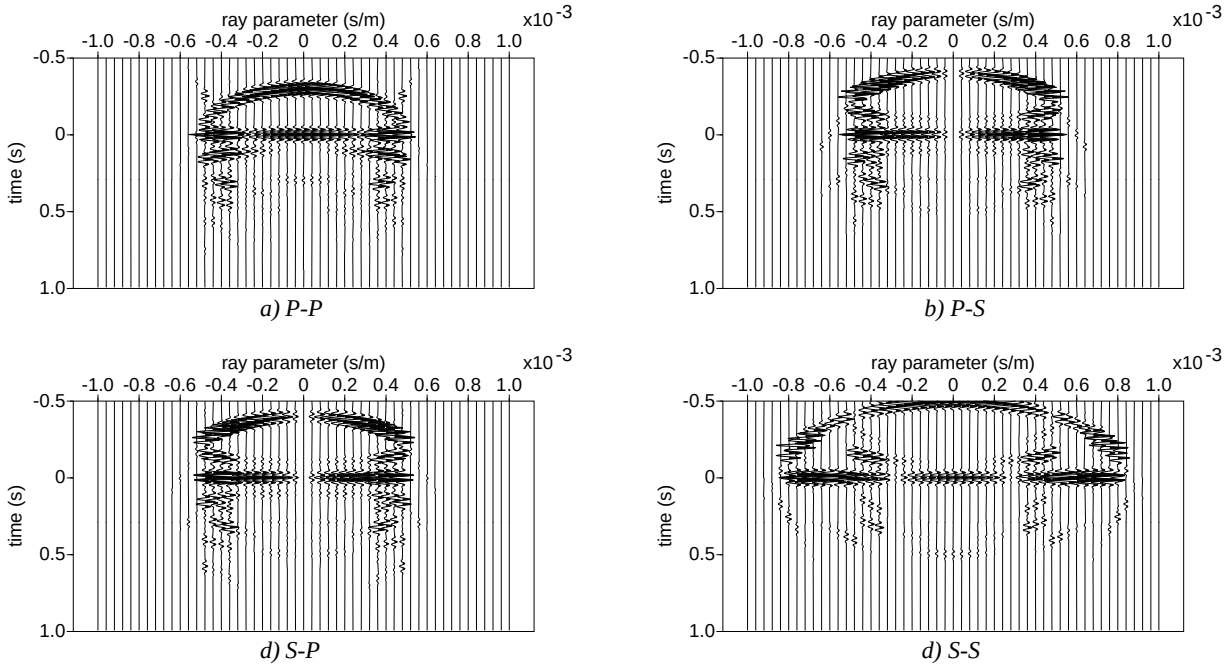


*a) P-P* *b) P-S*

*d) S-P* *d) S-S*

***Fig. 4:*** *$\tau$-p transformed gridpoint functions. Note that the angle-dependent reflection information occurs at $\tau = 0$.*

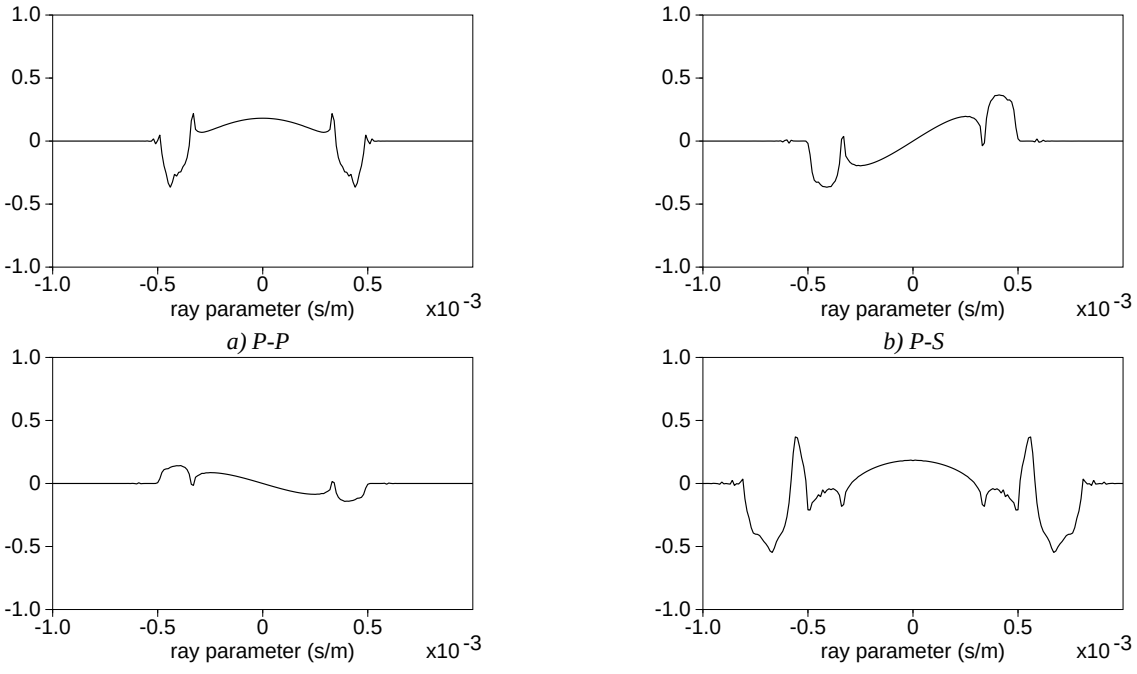


*a) P-P* *b) P-S*

*c) S-P* *d) S-S*

***Fig. 5:*** *The estimated angle-dependent reflection coefficients for one gridpoint on the second reflector, obtained by selecting amplitudes at zero intercept-time of the $\tau$-p transformed gridpoint functions in Fig. 4.*